Journal of Undergraduate Chemistry Research, **2026**, 25 (3), 86

PRELIMINARY SPECTROSCOPIC INVESTIGATION OF SUSPENDED NAPHTHALENE OVERLAYERS WITH INTERFACIAL VOIDS FORMED BY HEXANE UNDERLAYERS ON Al_2O_3

Mirabelle M. Smith*, Vanessa H. Kragelund*, Blake A. Bush* and A.M. Nishimura†

Department of Chemistry, Westmont College, Santa Barbara, CA 93108

Abstract

Bilayers were prepared on Al_2O_3 via the sequential physical vapor deposition of one of four hexane isomers followed by the deposition of a naphthalene overlayer. Molecular dynamics within the bilayers were monitored in real time by observing the fluorescence spectral signatures of naphthalene while the temperature of the Al_2O_3 was linearly ramped during the temperature programmed desorption (TPD) experiments. Desorption of the alkane underlayer created a voided space beneath the naphthalene overlayer and was accompanied by a spectral change associated with transient solvation of the naphthalene molecules. When the temperature increased sufficiently to overcome the activation barrier for the thermally induced collapse of the suspended overlayer, molecular reorganization occurred, resulting in enhanced excimer fluorescence. The magnitude of this enhancement was found to be related to the volume of the voided space. Because the surface area of the Al_2O_3 was fixed, the height of the voided space could be correlated with the effective height to which the alkane molecules extended normal to the surface. Utilizing this relationship, we propose estimates for the orientations and conformational geometries of the various alkane adlayers on Al_2O_3.

†Corresponding author: nishimu@westmont.edu *Undergraduate researchers and co-authors

Keywords: adsorption, naphthalene, hexane isomers, excimer, vapor deposition, desorption, TPD.
Submitted: June 23, 2026 Accepted: July 5, 2026 Revision received: July 5, 2026 Published: August 19, 2026

Introduction

In previous investigations of molecules vapor-deposited on Al_2O_3, the spectral signatures of aromatic fluorophores have been utilized to indirectly probe the surface morphology of alkane adlayers.[1-8] Naphthalene is particularly well-suited for this purpose; due to its planar molecular geometry, vapor-deposited naphthalene forms an amorphous solid in which electronically excited molecules readily assemble into excimers.[9] However, this excimeric formation can be disrupted, yielding monomers, if the naphthalene is solvated by an underlayer that percolates through the overlayer. This percolation occurs when the underlayer possesses a lower desorption temperature than naphthalene.

During temperature-programmed desorption (TPD) experiments, naphthalene undergoes a characteristic disorder-to-order phase transition at approximately 200 K.[1-8] This crystallization process can generate a high density of structural defect sites, particularly when the adlayer has experienced a severe degree of disorder prior to crystallization [1-8]—such as the structural disruption induced by the passage of underlayer molecules through the naphthalene overlayer. Consequently, these thermally induced molecular dynamics can be tracked and deduced via the spectral shifts and intensity changes in naphthalene fluorescence during a TPD ramp.[1-8]

As previously reported, the degree of disorder within the excimer phase scales with the volume of the void space remaining after the desorption of an n-alkane underlayer, which leaves behind a transiently suspended fluorophoric overlayer.[10,11] When the activation energy for the structural collapse of this suspended overlayer is thermally overcome, the ensuing molecular reorganization alters both the excimer emission intensity and the fluorescence intensity of the defect sites generated during the disorder-to-order transition.[10,11]

The present work investigates whether the intensities of either the excimer emission or the defect-site fluorescence can serve as sensitive probes to gain insight into the specific conformations and geometries of the underlying alkane adlayer. To test this hypothesis, the structural isomers of hexane were employed as underlayers, expanding upon the homologous series of *n*-alkanes investigated previously.[10] This approach holds the number of carbon atoms constant while systematically varying the molecular geometry and conformational flexibility of the underlayer. Ultimately, this allows us to evaluate the balance of dispersion interactions—which promote the aggregation and alignment of neighboring molecules—and adsorbate–substrate interactions on the Al_2O_3 surface, thereby enabling an estimation of the preferred conformations adopted by these interfacial adsorbates.

Experimental

Materials and Substrate Preparation

High-purity naphthalene and alkanes (> 99%) were purchased from commercial sources (Sigma-Aldrich, St. Louis, MO; TCI, Portland, OR) and used without further purification. The chemicals were loaded into a sample holder connected to a precision leak valve for controlled vapor deposition.

Experiments were performed in an ultra-high vacuum (UHV) chamber with a background hydrogen base pressure of 1 x 10^{-9} Torr. The substrate, a single-crystal Al_2O_3 (0001) (Crystal Systems, Inc., Salem, MA), was suspended from the lower end of a liquid nitrogen cryostat. It was mounted between two copper posts using a sapphire spacer to provide electrical isolation while maintaining partial thermal contact with the cryostat. Resistive heating of the Al_2O_3 substrate was achieved by passing electrical current through a thin tantalum foil placed in thermal contact with the crystal backface. The temperature was monitored using a type-K (chromel/alumel) thermocouple (Omega, Norwalk, CT) also in direct thermal contact with the substrate.

Temperature-Programmed Desorption (TPD)

Automated process control during TPD experiments was managed via a custom LabVIEW program (National Instruments, Austin, TX). The software utilized a proportional-integral-derivative (PID) feedback algorithm to linearly ramp the temperature of

the Al_2O_3 crystal at a rate of 1.98 ± 0.01 K s^{-1} (roughly 2 K s^{-1}).. To ensure a reproducible, clean surface, the substrate was flashed to 300 K after each experimental run; extended ramps to higher temperatures revealed no residual adsorbates.

Optical pumping of the adsorbed fluorophores was accomplished using a high-pressure Hg lamp. The lamp output was focused through a 0.25 m monochromator with the excitation wavelength λ_0 was set at 250 nm. Fluorescence emission from the adlayer on the Al_2O_3 surface was collected by a quartz lens and light pipe assembly, which routed the signal through a vacuum feedthrough to an ultraviolet-sensitive Ocean Optics SR2 UV-Vis spectrometer (Ocean Optics, Orlando, FL). During the TPD ramp, the LabVIEW program recorded full fluorescence spectra in real time every 300 ms. The resulting multi-dimensional data array was processed as a function of temperature using a custom MATLAB (MathWorks, Natick, MA) template to generate the wavelength-resolved TPD profiles presented herein.

Coverage Calibration

The LabVIEW system simultaneously interfaced with a residual gas analyzer (RGA) to monitor mass-spectrometric signals during both the deposition and desorption of naphthalene. Surface coverages Θ, expressed in monolayers (ML), were quantified by calibrating the integrated mass spectrometer peaks against independent optical interference experiments. This interference calibration provided accurate deposition rates with an estimated coverage error of ± 30% following procedures described in detail elsewhere[3].

Results

Following the methodology established previously in this series, the fluorescence spectrum of multilayer naphthalene served as the baseline for comparing all bilayer data.[10,11] Within the bilayer configuration, the alkane underlayers desorbed at temperatures below the desorption threshold of naphthalene. As the underlayer molecules desorbed and percolated through the fluorophoric overlayer, the naphthalene became transiently solvated, manifesting as characteristic monomer fluorescence. The onset of this monomeric emission was therefore utilized to precisely pinpoint the temperature range of underlayer desorption.

The physical dimensions of the void space evacuated beneath the naphthalene overlayer were inferred from the intensity of the excimer emission that emerged during structural reorganization. This reorganization occurred once the system gained sufficient thermal energy to overcome the activation barrier for the collapse of the suspended overlayer. Because larger voids accommodate a greater degree of molecular freedom and structural reorientation prior to collapse, the resulting excimer intensity serves as a reliable qualitative metric for the spatial volume of the void created beneath the naphthalene overlayer.

Complementing the enhanced excimer intensity, the trap (or defect-site) emission provides a qualitative measure of the structural disorder introduced during this macro-molecular reorganization.[10] This trap emission is intrinsically linked to lattice defects formed during the characteristic disorder-to-order phase transition of multilayer naphthalene.[10] Consequently, an elevation in trap emission intensity indicates that the physical collapse of the suspended overlayer, alongside its subsequent restructuring, induces additional defect sites or highly disordered domains within the crystalline naphthalene film.[10]

Multilayer naphthalene

Shown in Figure 1 is the wavelength-resolved TPD of naphthalene. The adlayer that formed was amorphous when naphthalene was vapor deposited on Al_2O_3. Optical pumping of the singlet electronic state gave rise to excimer fluorescence with λ_{max} = 398 nm that has been so categorized because of the observed broad and featureless spectrum.[9] As the temperature of the Al_2O_3 substrate was increased in a TPD experiment, naphthalene underwent a disorder-to-order transition commensing at about 190 K, at which temperature the spectrum changed to that observed for the monomer with two peaks at 325 and 334 nm. The doublet was due to the strong vibrational progression that has been attributed to a C-H bending vibration.[9] The maximum monomer intensity occurred at 205 K and desorption occurred at about 210 K.

2-Methylpentane/naphthalene

Shown in Figure 2 is the wavelength-resolved TPD of a bilayer of 2-methylpentane and naphthalene. 2-Methylpentane desorbed at about 134 K. The enhanced excimer intensity occurred at 398 nm and at about 152 K during the TPD, whereas the peak intensity of the trap occurred at 197 K and λ_{max} = 326 nm. The 2-methylpentane's effect on the excimer was delayed by about 26

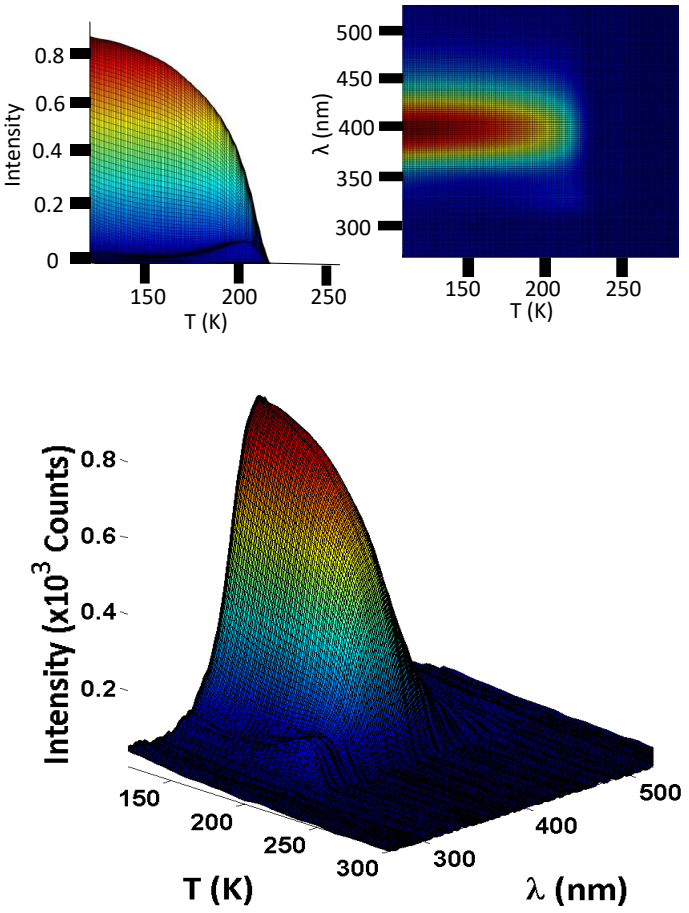

Figure 1. Wavelength-resolved TPD of naphthalene neat with coverage of 87 ML. The excimer has a λ_{max} = 398 nm. The disorder-to-order transition occurs at 205 K during the TPD, but the trap emission from the ordered state is barely visible. Left inset: Fluorescence intensity vs. T during the TPD. Right inset: top view.

K. A plot of both the enhanced excimer intensity and the intensity of the trap are shown in Figure S1. Here, the leveling of the slope occurred at around ~2 $\Theta_{2\text{-methylpentane}}$(ML)/ $\Theta_{naphthalene}$(ML) ML coverages and that the excimer and trap intensities were correlated is shown in Figure S4.

3-Methylpentane/naphthalene

Shown in Figure 3 is the wavelength-resolved TPD of a bilayer of 3-methylpentane and naphthalene. The peak desorption temperature for 3-methylpentane was about 140 K. The enhanced excimer intensity occurred at about 156 K, and the peak intensity of the trap was observed at 204 K. The temperature interval between the desorption of 3-methylpentane and the maximum excimer intensity was about 16 K. A plot of the enhanced excimer intensity and the intensity of the trap is given in Figure S2 and that the intensites of the excimer and trap are correlated is shown in Figure S5. Here, the leveling of the slope occurred at around 2 $\Theta_{3\text{-methylpentane}}$(ML)/ $\Theta_{naphthalene}$(ML).

2,3-Dimethylbutane/naphthalene

Shown in Figure 4 is the wavelength-resolved TPD of a bilayer of 2,3-methylpentane and naphthalene. The desorption temperature for 2,3-methylpentane was about 132 K. The compact geometrical conformer resulted in minimal evidence during desorption. At about 127 K, a peak at 330 nm due to solvation of naphthalene as the 2,3-dimethylbutane desorbed through.The disorder-to-order transition was observed at 204 K with λ_{max} at 330 nm. A plot of the enhanced excimer intensity and the intensity of the trap is given in Figure S3. Here, the leveling of the maximum excimer intensity as a function of coverage slope occurred at around 1.4 $\Theta_{2,3\text{-dimethylbutane}}$(ML)/ $\Theta_{naphthalene}$(ML). The plot of the maximum trap fluorescence

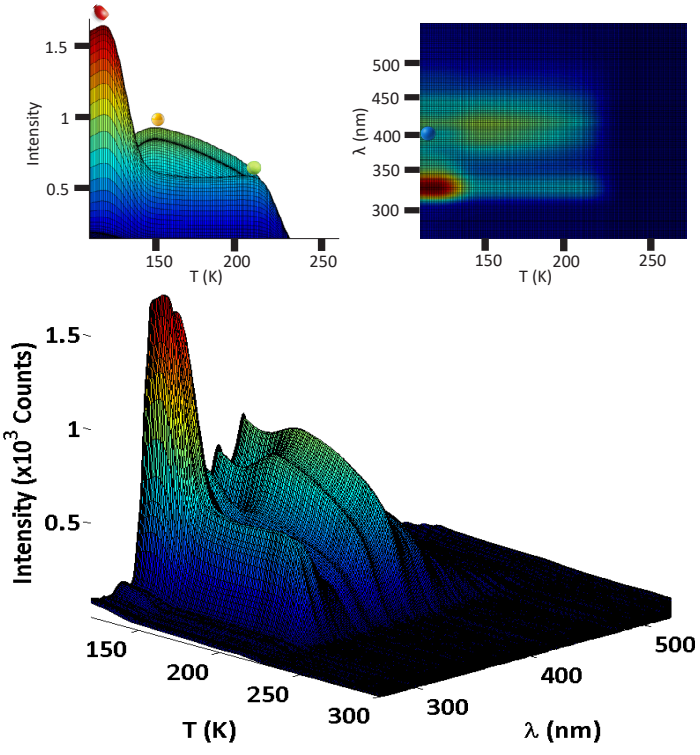

Figure 2 Wavelength-resolved TPD of naphthalene with $\Theta_{naphthalenel}$ = 85 ML with an underlayer of 2-methylpentane with $\Theta_{2\text{-methylpentane}}$ = 148 ML Blue and red balls point to the initial excimer fluorescence and solvated monomer intensities, respectively. Yellow and green balls point to the maximum excimer and trap intensities, respectively. Left inset: fluorescence intensity vs T during the TPD. Right inset: top view.

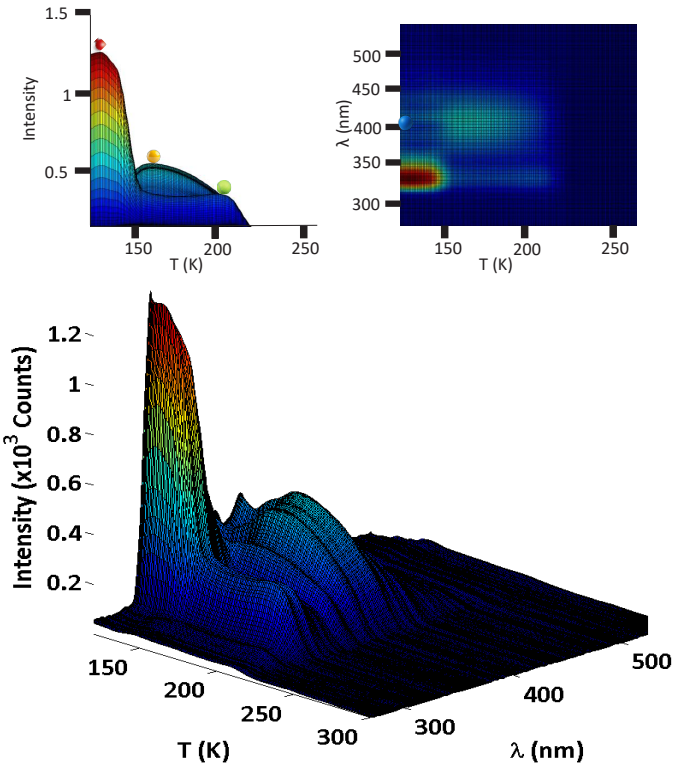

Figure 3. Wavelength-resolved TPD of naphthalene with $\Theta_{naphthalenel}$ = 102 ML with an underlayer of 3-methylpentane with $\Theta_{3\text{-methylpentane}}$ = 108 ML. Blue and red balls point to the initial excimer fluorescence and solvated monomer intensities, respectively. Yellow and green balls point to the maximum excimer and trap intensities, respectively. Left inset: fluorescence intensity vs T during the TPD. Right inset: top view.

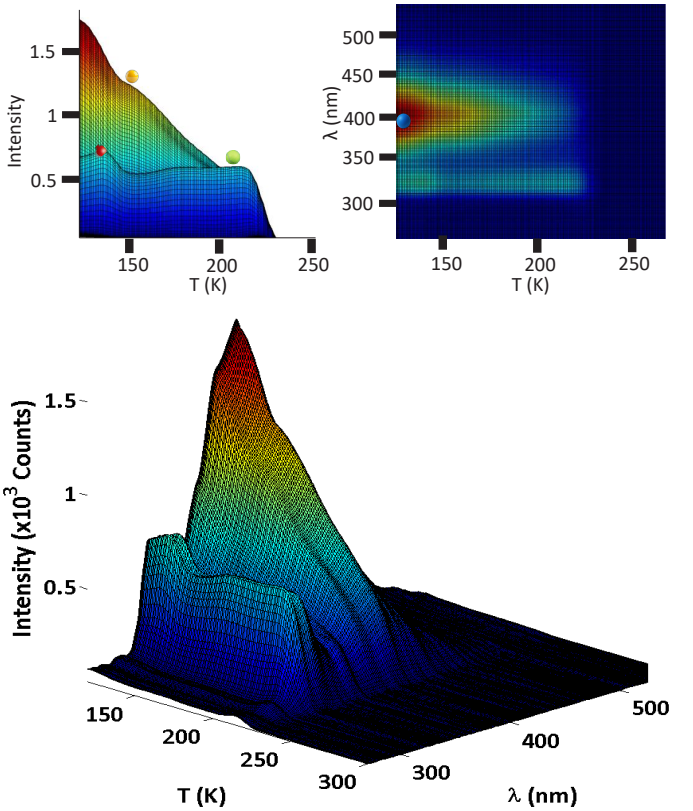

Figure 4. Wavelength-resolved TPD of naphthalene with $\Theta_{naphthalenel}$ = 103ML with an underlayer of 2,3-dimethylbutane with $\Theta_{2,3\text{-dimethylbutane}}$ = 150ML. Blue and red balls point to the initial excimer fluorescence and solvated monomer intensities, respectively. Yellow and green balls point to the maximum excimer and trap intensities, respectively. Left inset: fluorescence intensity vs T during the TPD. Right inset: top view.

as a function of coverage appears to level at about 1.6 $\Theta_{2,3\text{-dimethylbutane}}$(ML)/ $\Theta_{naphthalene}$(ML) coverages. That the intensities of the excimer and the trap are correlated is shown in Figure S6.

2-Methylbutane/naphthalene

Shown in Figure 5 is the wavelength-resolved TPD of a bilayer of 2-methylbutane and naphthalene. The desorption temperature for 2-methylbutane is about 117 K.

Discussion

In the introduction, the following question was raised: if the temperatures corresponding to the maxima in excimer fluorescence intensity were known and if the lengths of the various hexane isomers projected normal to the Al_2O_3 surface were also known, do these two variables correlate? Such a correlation would be expected if the maxima in the excimer intensity arose from molecular reorganization of naphthalene following the collapse of a suspended overlayer. Because the Al_2O_3 single crystal provides a fixed surface area, the primary variable defining the volume of the void space created by underlayer desorption is its height. Under this model, the maximum excimer intensity should scale proportionally with the height of the void generated by the desorbing alkane underlayer. This height, in turn, is determined by the molecular geometry and orientation of the adsorbed alkane molecules.

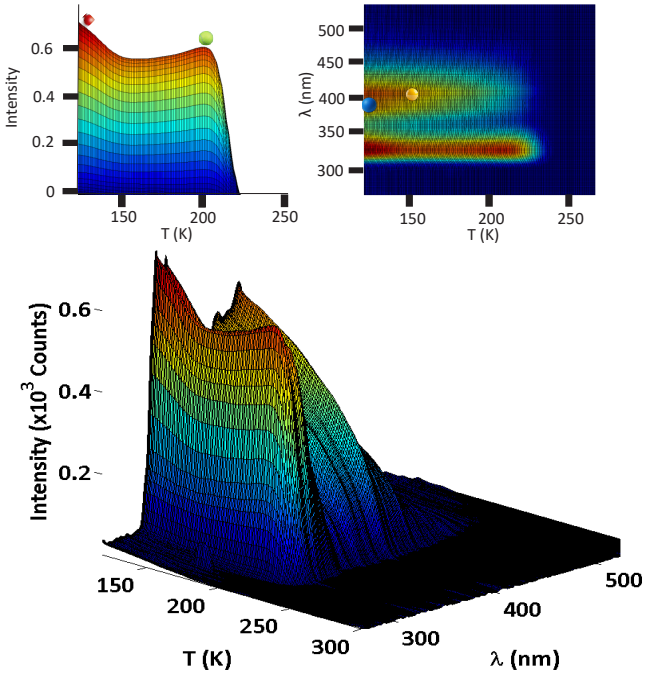

Figure 5. Wavelength-resolved TPD of naphthalene with $\Theta_{naphthalenel}$ = 95ML with an underlayer of 2-methylbutane with $\Theta_{2\text{-methylbutane}}$ = 151ML. Blue and red balls point to the initial excimer fluorescence and solvated monomer intensities, respectively. Yellow and green balls point to the maximum excimer and trap intensities, respectively. Left inset: fluorescence intensity vs T during the TPD. Right inset: top view.

Figure 6 is a summary of the fluorescence intensities of naphthalene measured at various significant points during the TPD with the alkanes that were involved in this study. In addition, this expanded summary includes all of the alkanes that were involved in the previous experiments in this series.[10]

The dispersion interactions that must be considered for the alkane underlayers are: (a) those between the alkane molecules and the Al_2O_3 surface, which is polar whereas the alkanes are nonpolar, and (b) those between neighboring alkane molecules. Intermolecular interactions that promote aggregation of the alkanes have been shown to cause *n*-pentane and *n*-hexane to adopt orientations approximately normal to the Al_2O_3surface in the coverage regime studied here.[12,13] To maximize intermolecular dispersion interactions, these two alkanes were assumed to possess carbon–carbon bonds entirely in the anti conformation.[12,13]

As the carbon chain length increases, however, the statistical probability of adopting one or more gauche conformations also increases.[14] Consequently, it is reasonable to propose that *n*-heptane and *n*-octane contain one, two, or even three C–C bonds in the gauche conformation.[14] Standard bond lengths of 1.54 Å for an sp^3–sp^3 C–C bond and 1.10 Å for an sp^3–H bond were used in constructing the molecular models.[15] Using these parameters, models containing two gauche C–C bonds yielded effective mo-

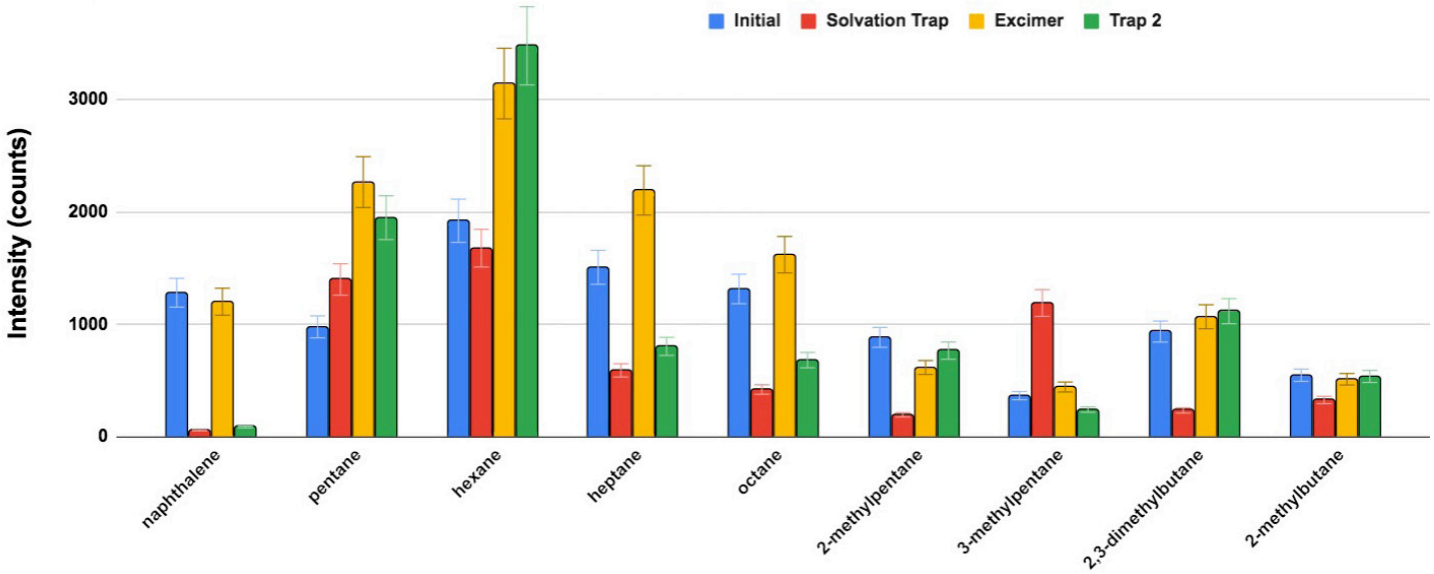

Figure 6. Summary of the average fluorescence intensity initially, maximum excimer intensity and subsequent trap emission intensity after the disorder-to-order transition for the various alkane underlayers. Intensities were averaged past the leveling of the slopes in Figs. S1, S2 and S3. Intensities for the homologous series from pentane to octane are from ref 10.

lecular projection heights normal to the surface of approximately 5.5 Å for *n*-heptane and 6.0 Å for *n*-octane (Cf. S10).

The branched hexane isomers were estimated to occupy substantially smaller dimensions normal to the surface. 2,3-Dimethylbutane possesses a nearly spherical geometry with an effective diameter of approximately 4.0 Å. The effective height of 2-methylpentane was estimated to be 4.7 Å. For 3-methylpentane, an effective height of 3.8 Å was assigned by assuming that the molecule favors interactions with the polar Al_2O_3 surface slightly more than intermolecular aggregation, while its kinked geometry increases dispersive contact with neighboring molecules. Finally, the effective height of 2-methylbutane was estimated to be 3.6 Å, calculated as the average of a four-carbon profile (3.0 Å) and a three-carbon profile (4.1 Å) resting on the surface. The branched isomers exhibited significantly smaller dimensions normal to the surface:

Using these estimated molecular dimension, the effective dimensions of the alkane molecules normal to the Al_2O_3 surface were plotted as a function of the observed maximum excimer fluorescence intensities, and the results are shown in Figure 7. The data correspond to a naphthalene overlayer coverage of approximately 100 ± 25 ML. The best-fit line yielded a slope of 0.0012 Å/count and an intercept of 3.5 Å, with an R^2 value of 0.87. Under these conditions, namely for a naphthalene overlayer coverage of approximately 100 ML, the measured enhancement in the excimer fluorescence intensity can be used to estimate the effective height of an alkane underlayer normal to the Al_2O_3 surface. Consequently, the enhanced excimer fluorescence intensity may serve as an indirect probe of the molecular geometry of alkane adlayers, allowing the effective orientation and conformation of the adsorbed molecules to be estimated.

A complementary interpretation considers initial fluorescence quenching is mediated by proximity to the Al_2O_3 surface.[16] If the initial fluorescence intensity reflects the average separation of the naphthalene molecules from the substrate before TPD begins, then the initial fluorescence intensities shown in Figure 6 as 'initial' should also correlate with the alkane underlayer height. For this plot shown in Figure 8, the trendline yielded a slope of 0.0023 Å/count with an intercept of 3.1 and $R^2 = 0.85$.

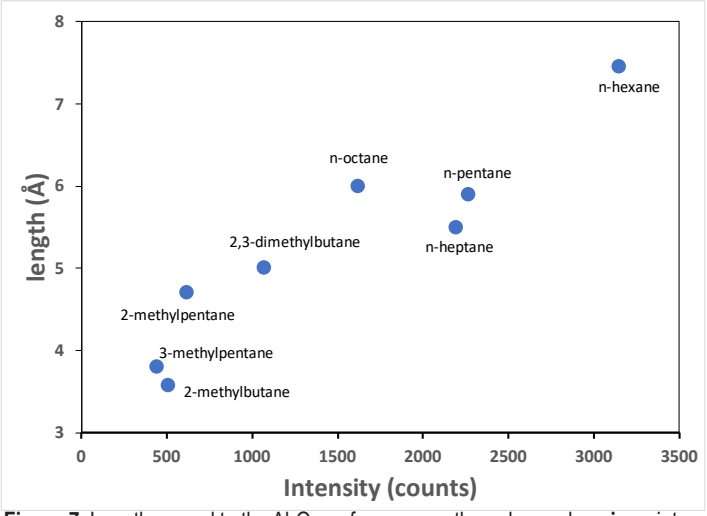

Figure 7. Length normal to the Al_2O_3 surface versus the enhanced **excimer** intensity given in Figure 6. Trendline gave y = 0.0012 x + 3.5 with $R^2 = 0.87$.

The weakest correlation was obtained by comparing the effective heights with the fluorescence intensity of the defect emission that develops during the disorder-to-order phase transition, designated as Trap 2 in Figure 6. The corresponding plot is shown in Figure 9. This lower reliability is expected because the disorder-to-order transition is governed by nucleation and crystallization pathways. These processes are inherently stochastic, introducing substantial statistical scatter into the measured trap intensities and resulting in the lowest R^2 value among the evaluated metrics. It is notable that *n*-octane exhibits a systematic positive deviation and acts as an outlier in this plot. This suggests that the two-gauche molecular model for *n*-octane may be incomplete; a conformation incorporating three gauche C–C bonds would reduce its calculated height, offering a better fit to the correlation and a more accurate representation of the adlayer structure.

The agreement between the slopes obtained for *n*-pentane[10] and *n*-hexane[10] and the overall trendline slopes in Figures 7–10 lends further credibility to the estimated molecular distances normal to the surface, as the orientations of these molecules on Al_2O_3 are already known from previous studies.[10] These trendlines may provide a means of refining the estimated distances normal to the

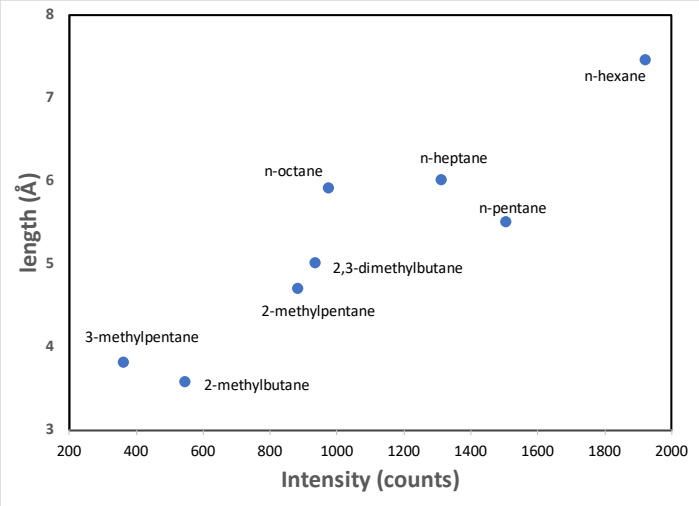

Figure 8. Length normal to the Al_2O_3 surface versus **initial** intensity prior to the TPD experiment as given in Figure 6. Trendline gave y = 0.0023 x + 3.1 with $R^2 = 0.85$.

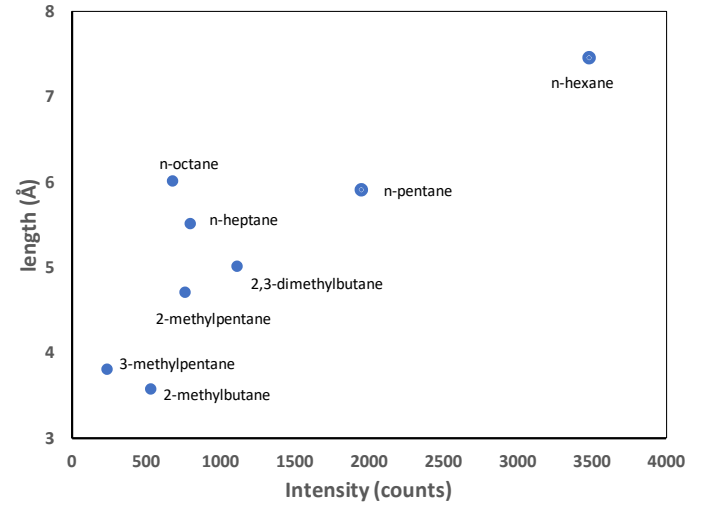

Figure 9. Length normal to the Al_2O_3 surface versus **trap 2** intensity during the TPD experiment as given in Figure 6. Trap 2 is the monomer fluorescence subsequent to the disorder-to-order transition. Trendline gave y = 0.001 x + 4.0 with $R^2 = 0.70$.

surface for the alkane adlayers. In particular, the systematic positive deviation of *n*-octane suggests that its molecules may adopt additional gauche conformations, thereby reducing the effective molecular height above the surface.

The same analyses were done with biphenyl overlayer as had been done in a previous study with the same underlayer. The wavelength-resolved TPD's are shown in S7-S9. Shown in Figure 10 are the results that includes data from ref. 11. The trendline showed a reasonable fit with $R^2 = 0.64$, but some outliers did appear, particularly *n*-octane.

The potential application of this approach is illustrated by preliminary experiments involving cyclohexane. For approximately 180 ML of cyclohexane covered by about 150 ML of naphthalene, the enhanced excimer fluorescence intensity, when substituted into the trendline equation derived from the excimer data in Figure 6, yielded an effective height normal to the surface of 4.3 Å. For comparison, the molecular dimension of cyclohexane is approximately 5.1 Å when oriented perpendicular to the Al_2O_3 surface with maximum intermolecular attraction due to dispersion and about 2.8 Å when lying parallel to the surface wherein the interaction between the surface and cyclohexane is a maximum. The experimentally determined value therefore suggests that the cyclohexane molecules adopt an average orientation of approximately 45° with respect to the surface normal. At the coverages employed in this study, the cyclohexane adlayer would be expected to be multilayer in nature. Because the cyclohexane coverage used in these experiments produced a multilayer film, the calculated value should be interpreted as an *average* projection normal to the surface rather than a unique orientation adopted by every molecule.

In Figure 6, what is labeled as solvation trap corresponds to the monomer fluorescence that develops as the desorbing alkane underlayer percolates through the naphthalene overlayer. Solvation arises from dispersion interactions between the alkane molecules and naphthalene and is expected to be most effective when the alkane adopts the extended anti conformation, which maximizes molecular contact.[18] Consequently, the observed increase in monomer fluorescence intensity is expected to reflect the extent to which the anti conformation is favored over gauche conformations. With the exception of 3-methylpentane, the solvation-trap intensities closely parallel the trends observed for the maximum excimer fluorescence, supporting the interpretation that molecular conformation plays an important role in both phenomena.

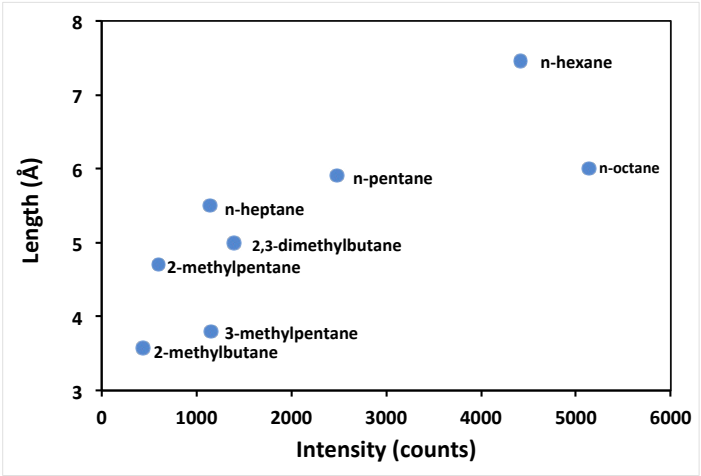

Figure 10. Length normal to the Al_2O_3 surface versus **trap** intensity during to the TPD experiment for **biphenyl** overlayer as given in Figures S7-S10. Trap 2 is the monomer fluorescence Trendline gave y = 0.0006 x + 4.1 with $R^2 = 0.64$. Data for n-alkanes were from Ref. 11.

In conclusion, while portions of this structural analysis remain preliminary, the experimental data provide strong qualitative support for the proposed void-space/suspended-adlayer model. Although the optical method outlined here yields a primary, one-dimensional estimation of effective underlayer height normal to the substrate, pairing these measurements with reasonable conformational assumptions enables the determination of an approximate three-dimensional picture of organic adlayer orientation. Future studies will integrate this void-space model into the routine analysis of overlayer fluorescence data to describe the morphology, alignment, and molecular organization of broad range of alkane adlayers deposited on Al_2O_3 surfaces.

Acknowledgment

The authors would like to thank the John Stauffer Charitable Trust for funding the student stipends for summer research. This work was supported by the donors of ACS Petroleum Research Fund under Undergraduate Research #68385-UR5 .

References

1. B.X. Moses, C.D. Tobey, A.O. Lopez and A.M. Nishimura, *JUCR*, **2025**, 24, 66-72.
2. I.Z. Song, S.T. Watanabe and A.M. Nishimura, *JUCR*, **2023**, 22, 78-85.
3. M.K. Condie, B.D. Fonda, Z.E. Moreau and A.M. Nishimura, *Thin Solid Films*, **2020**, 697, 137823-137828.
4. A.O. Lopez, B.X. Moses, C.D. Tobey, J. Arrieta, M. Ticas, J. Zerwas amd A.M. Nishimura, *JUCR*, **2025**, 24, 59-65.
5. B.D. Fonda, Z.I. Shih, J.J. Wong, L.G. Foltz, K.A. Martin and A.M. Nishimura, *JUCR*, **2018**, 17, 32-35.
6. K.L. Nili, Z.E. Moreau and A.M. Nishimura, *JUCR*, **2020**, 19, 19-23.
7. M.K. Condie, Z.E. Moreau and A.M. Nishimura *JUCR*, **2019**, 18, 15-18.
8. M.K. Condie, C. Kim, Z.E. Moreau, B. Dionisio, K. Nili, J. Francis, C. Tran, S. Nakaoka and A.M. Nishimura, *JUCR*, **2020**, 19, 14-17.
9. J.B. Birks. *Photophysics of Aromatic Molecules*, John Wiley & Sons Ltd., New York, NY (**1970**), pp. 301-370.
10. V. Kragelund, B. Bush, M. Smith and A.M. Nishimura, submitted to JUCR.
11. B. Bush, M. Smith, V. Kraglund and A.M. Nishimura, submitted to JUCR
12. C.M. Aubuchon, B.S. Davison, A.M. Nishimura and N.J. Tro, *J. Phys Chem.* **1994,** 98, 240-244.
13. R.M. Slayton, C.M. Aubuchon, T.L. Camis, A.R. Noble and N.J. Tro. *J. Phys. Chem*., **1995**, 99, 2151-2154.
14. T. Tynkkynen, T. Hassien, M. Tiainen, P. Soininen, R. Laatikainen, *Magnetic Resonance In Chemistry*, **2012**, 50, 598-607
15. Wikipedia https://en.wikipedia.org/wiki/Bond_length.
16. D.R. Haynes, K.R. Helwig, N.J. Tro and S.M. George, *J. Chem. Phys.* **1990**, 93, 2836-2847.
17. K. Kojima, Prog. Crystal Growth and Charact. **1991**, 23, 369-420.

18. M. Lamotte, J. Joussot-Dubien, M.J. Mantione and P. Claverie, *Chem. Phys. Lett.* **1974**, 27, 515-520.

Supplemental Material

Normalized intensities of the excimer and traps as function of the ratio of alkane (ML)/naphthalene (ML): S1-S3

To show that at a certain coverage of the alkane, the intensity leveled off. The leveling off point is where the underlayer completely affected the naphthalene layer such that additional passage of the underlayer had no further affect.

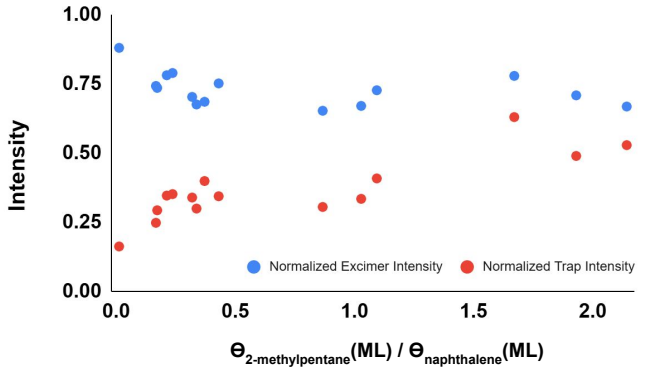

Figure S1. Normalized intensities of excimer and trap as functions of the ratio of 2-methypentane and naphthalene coverages. Plot of the transmittance of bilayer with varying 2-methylpentane as a function of $\Theta_{2\text{-methylpentane}}/\Theta_{naphthalenel}$ $\Theta_{biphenyl}$ .held constant at 91 ± 12 ML.

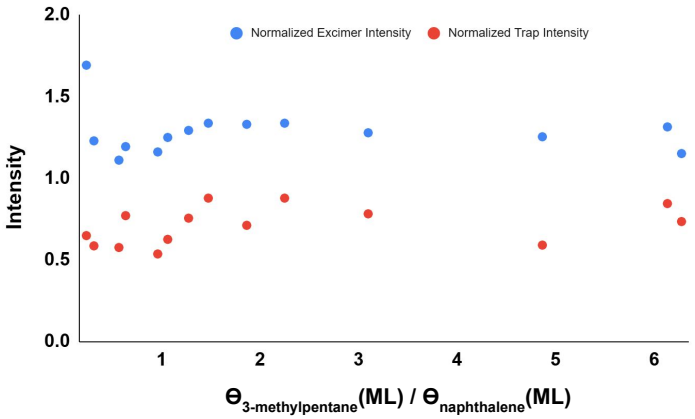

Figure S2. Normalized intensities of excimer and trap as functions of the ratio of 3-methypentane and naphthalene coverages. Plot of the transmittance of bilayer with varying 3-methylpentane as a function of $\Theta_{3\text{-methylpentane}}/\Theta_{naphthalenel}$. $\Theta_{naphthalene}$ held constant at 112 ± 30 ML.

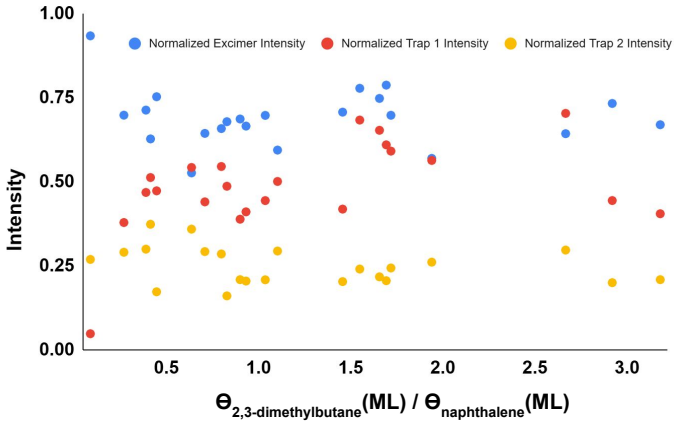

Figure S3 Normalized intensities of excimer and trap as functions of the ratio of 2,3-dimethybutane and naphthalene coverages. Plot of the transmittance of bilayer with varying 2,3-dimethylbutane as a function of $\Theta_{2,3\text{-dimethylebutane}}/\Theta_{naphthalenel}$

Correlation of the fluorescence intensities due to the naphthalene trap and excimer intensities: S4-S6

To show that the trap intensity was correlated to the excimer,

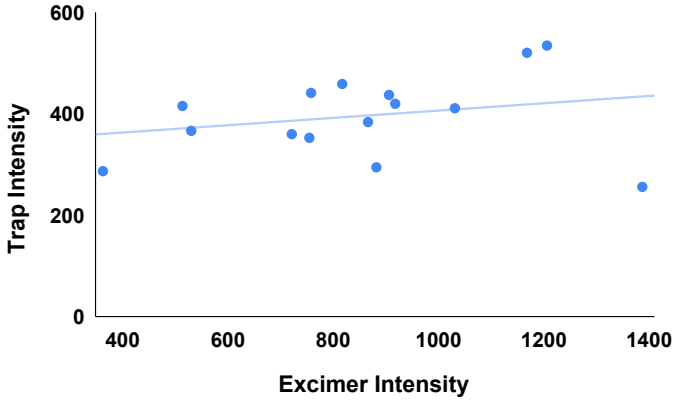

Figure S4. Plot of the fluorescence intensity of the excimer at 398 nm at 153 K and the trap at 326 nm at 197 K as a function of $\Theta_{2\text{-methylpentane}}$ with $\Theta_{naphthalenel}$ = 91 ±12 ML that had been deposited at 117 K with an underlayer of 2-methylpentane. Trendline had a slope of 0..64.and R^2 = 0.79

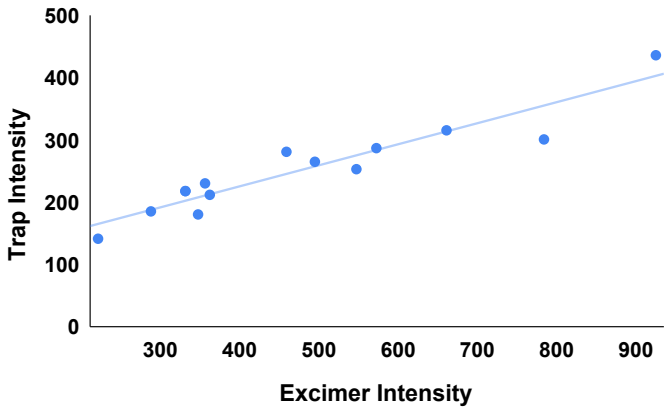

Figure S5. Maximum trap intensity as a function of maximum excimer intensity for various 3-methylpentane/naphthalene coverages. This is an indicator that the two intensities are correlated. $\Theta_{naphthalene}$ = 112± 30 ML. Slope = 0.34; R^2 = 0.88

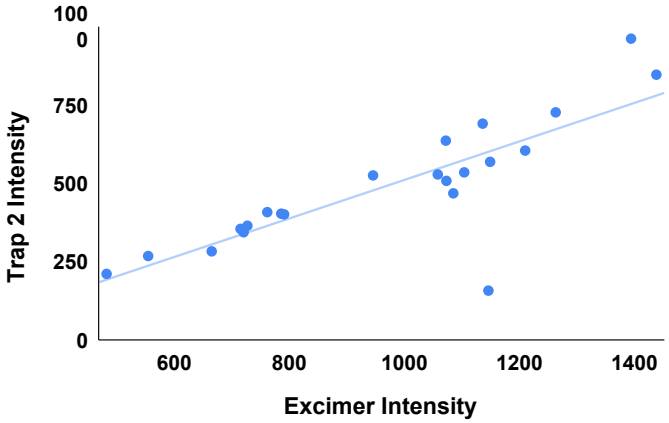

Figure S6. Maximum trap intensity as a function of maximum excimer intensity for various 2,3-dimethylbutane/naphthalene coverages. This is an indicator that the two intensities are correlated. $\Theta_{naphthalene}$ = 104 ± 14 ML. Slope = 0.62; R^2 =0.66

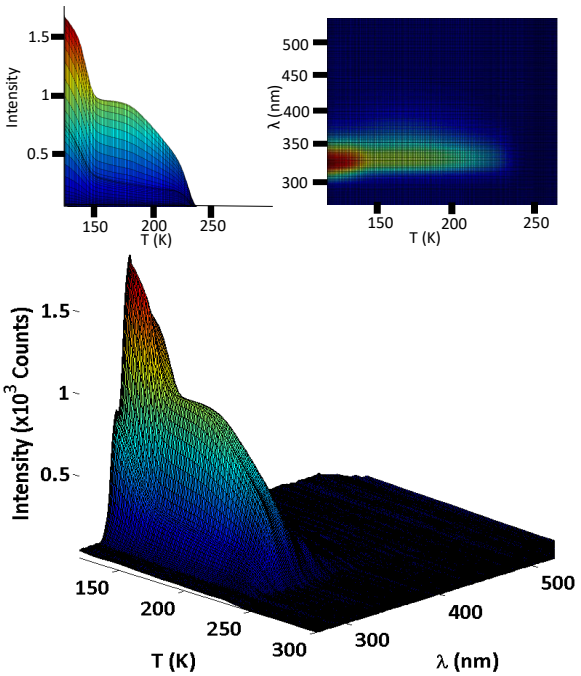

Figure S7. Wavelength-resolved TPD of biphenyl with $\Theta_{biphenyl}$ = 101ML with an underlayer of 2-methylpentane with $\Theta_{2\text{-methylpentane}}$ = 150ML. Left inset: fluorescence intensity vs T during the TPD. Right inset: top view.

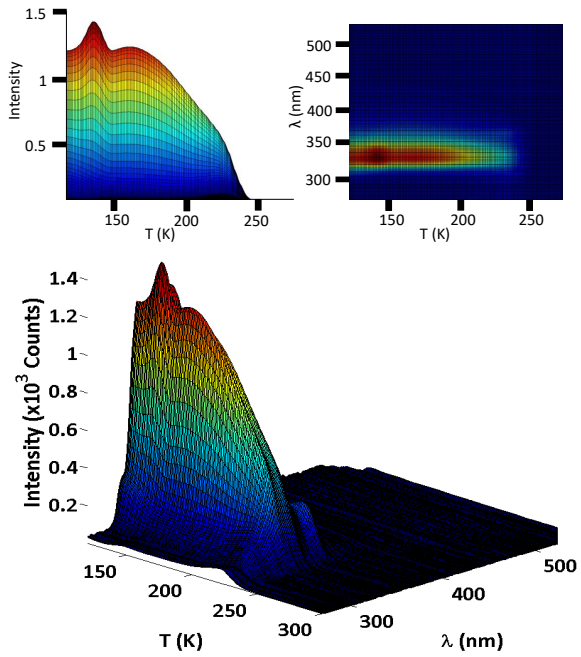

Figure S8. Wavelength-resolved TPD of biphenyl with $\Theta_{biphenyl}$ = 116ML with an underlayer of 3-methylpentane with $\Theta_{3\text{-methylpentane}}$ = 110ML. Left inset: fluorescence intensity vs T during the TPD. Right inset: top view.

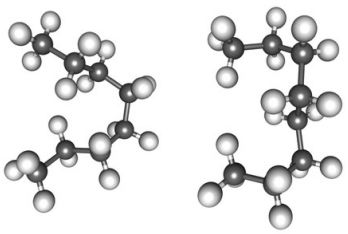

Figure S10. Conformers of n-Octane with one gauche (L) C-C bond and two gauche (R) C-C bonds.

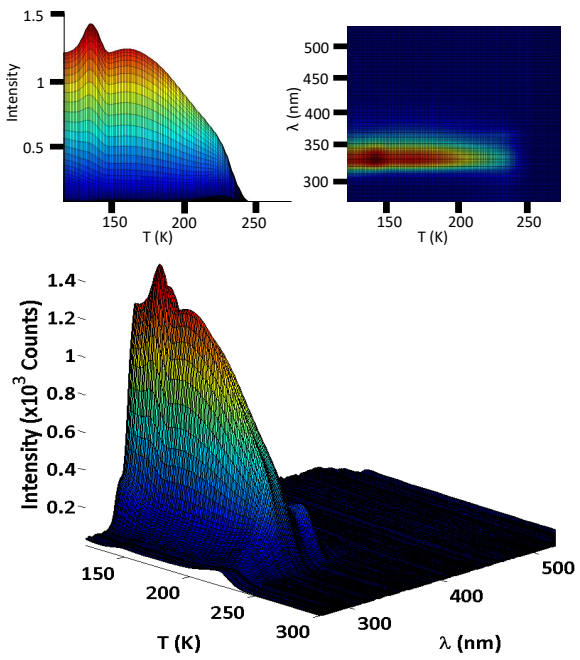

Figure S9. Wavelength-resolved TPD of biphenyl with $\Theta_{biphenyl}$ = 116ML with an underlayer of 2,3-methylpentane with $\Theta_{2,3\text{-methylbutane}}$ = 109ML. Left inset: fluorescence intensity vs T during the TPD. Right inset: top view.